Carrier Lifetimes and Influence of In-Grown Defects in N-B Co-Doped 6H-SiC

2014 IOP Conf. Ser.: Mater. Sci. Eng. 56 012004

(http://iopscience.iop.org/1757-899X/56/1/012004)

IOP Conf. Series: Materials Science and Engineering **56** (2014) 012004 doi:10.1088/1757-899X/56/1/012004

Carrier Lifetimes and Influence of In-Grown Defects in N-B Co-Doped 6H-SiC

V Grivickas[1], K Gulbinas[1], V Jokubavičius[2], J W Sun[2], M Karaliūnas[1], S Kamiyama[3], M Linnarsson[4], M Kaiser[5], P Wellmann[5] and M Syväjärvi[2]
[1]Institute of Applied Research, Vilnius University, Saulėtekio av. 10, Vilnius, 10223 Lithuania
[2]Department of Physics, Chemistry and Biology, Linköping University, Linköping, 58183 Sweden
[3]Faculty of Science and Technology, Meijo University, Tempaku-ku, Nagoya, 468-8502 Japan
[4]School of Information and Communication Technology, Royal Institute of Technology, Kista-Stockholm, 58183 Sweden
[5]Department of Materials Science – Materials for Electronics and Energy Technology, University of Erlangen-Nuremberg, Erlangen, 91058 Germany

E-mail: vytautas.grivickas@ff.vu.lt

Abstract. The thick N-B co-doped epilayers were grown by the fast sublimation growth method and the depth-resolved carrier lifetimes have been investigated by means of the free-carrier absorption (FCA) decay under perpendicular probe-pump measurement geometry. In some samples, we optically reveal in-grown carbon inclusions and polycrystalline defects of substantial concentration and show that these defects slow down excess carrier lifetime and prevent donor-acceptor pair photoluminescence (DAP PL). A pronounced electron lifetime reduction when injection level approaches the doping level was observed. It is caused by diffusion driven non-radiative recombination. However, the influence of surface recombination is small and insignificant at 300 K.

1. Introduction

B and N co-doped 6H-SiC epilayers combined with GaN-ultraviolet excitation chip can be used as an active material in a high-efficiency LED structure stack for a visible broad spectral light generation by DAP emission mechanism [1,2]. As accounted theoretically, this concept from blue excitation light could provide internal energy conversion up to 70% with a high color quality of a white spectrum. Moreover, in SiC it is possible to obtain uniform concentration of impurities in depth of hundred microns. It is well known that SiC material itself has excellent thermal conductivity property which is important for high power LED performance. Therefore, high co-doping in SiC requires further understanding of the growth techniques and investigation of optical properties. Up to now, very little is known on impurity clustering, on actual carrier transport mechanism and on the competing nonradiative recombination channels [3, 4]. In addition, an impact of co-doped acceptor situated on the hexagonal and the cubic sites in 6H-SiC matrix and their influence in the DAP processes is also not completely established yet [5].

In this work we present the free-carrier-absorption (FCA) lifetime studies performed on thick N-B doped epilayers in order to elucidate influence of surface and bulk recombination. We focus on previously observed pronounced injection dependence of the carrier lifetimes [3]. The surface recombination is estimated by performing the depth-resolved FCA measurement. Furthermore, we

examine overall carrier lifetime dependence on the concentration of in-grown threadlike defects and show that the only samples with low density of these defects exhibit DAP photoluminescence.

2. Experimental

The N-B doped 6H-SiC samples were grown by the fast sublimation growth method on low-off-axis 6H-SiC commercial substrates using N and B doped PVT crystalline SiC as a source material. The N

Table 1. Two types of doped 6H-SiC epilayers were studied (denoted ELS and RF batches).

Sample	ELS296	ELS297	RF18	RF04
Epilayer [μm]	200	200	130	110
B [cm^{-3}]	$2.1 \cdot 10^{18}$	$4 \cdot 10^{16}$	$2.5 \cdot 10^{18}$	$2.2 \cdot 10^{18}$
N [cm^{-3}]	$1.3 \cdot 10^{19}$	$1.1 \cdot 10^{19}$	$4 \cdot 10^{18}$	$8 \cdot 10^{18}$
Defects [cm^2]	10^{1} *a)	10^{6} *a)	10^{1}-10^{2} *b)	10^{5} *b)
Lifetime (μw-PC) [μs]	-	-	0.8	0.22
Lifetime component (FCA) [μs]	1.5 50	0.18	3 150 1200	0.1

*a) carbon inclusions; *b) polycrystalline inclusions

concentration was also enhanced by the N gas ambient during the growth [1]. Intentionally, the samples were grown to have higher donor concentration than acceptor concentration because the overcompensated *n*-type 6H-SiC provides more efficient DAP photoluminescence [1]. Estimated doping inhomogeneity varied about 20 - 30% along growth direction [see Gulbinas et al. in this issue]. Thickness of the epilayer was between 110 to 200 μm. The N and B concentrations, as determined by secondary ion mass spectrometry profiles, are provided in table 1. Unfortunately, it is not known how boron distributes between deep (dB) and shallow (sB) boron energy levels.

After growth the samples were cut into 0.5-0.7 mm-wide strips and lateral strips facets were polished to optical quality. The samples were inspected by Nomarsky microscope. The images of cross section view under polarized light showed in-grown defects with density varying widely from 10^1 cm^2 to 10^6 cm^2 (table 1). Side view revealed that thin filamentary defects were spreading out in groups along some straight line directions, like in figure 1a, and as a single defect, like in figure 1c. Top view, figure 1b, shows variety of directions along which the lines are able to spread. Closer inspection revealed that these filaments are composed of smaller dots. The alignment of the defects in the direction perpendicular to the interface implies that these defects are extended primarily along the threading dislocations. In the high defect density samples (RF-batch samples) it was found that the most of filamentary defects collapse into elliptical cones. Figures 1d, e show that those defects probably contain a polycrystalline SiC. Carbon concentration was determined by X-ray element analysis. It showed that these defects contain of 65-75 % carbon inside the cone. The cone defects appear visible on the surface top view as a phase inclusion of a 5-30 μm in size as shown in figure 1f. It is interesting to note that only in 10-20% of these cases cone defects are originating from the substrate/epilayer interface. In the rest 80-90% cases, they originate (or became visible) at a certain depth within the epilayer. This implies that suppression of defect growth might be achieved by a proper control of the growth conditions.

Technical details about the spatially and time-resolved FCA detection technique can be found in a review chapter [6]. For the carrier lifetime studies free carriers were excited by 2 ns laser pulses at 355 nm wavelength of the third harmonic from a YAG laser. The diameter of laser spot was about 1 mm^2, and the pulse repetition rate was equal to 40 Hz. If needed, the pump pulse fluence was reduced by optical filters. The induced FCA transient, $\Delta\alpha(t) = 1/d \cdot \ln(T_0/T(t))$, was detected at different depths by using 1.3 μm cw-probe beam which was directed perpendicular to the excited surface. The probing depth-resolution is set by the diameter of the probe beam within the crystal which was estimated to be about 7 μm. Using micrometer translation of the cryostat together with sample it was possible to choose the position of the probe beam with 1 μm precision at any distance from the excited surface. The transmitted probe beam was collected by lenses and optical transient was recorded by a fast

photoreceiver with 0.5 ns time resolution. Then the probe decay was averaged by the digital oscilloscope over typically 500 traces in order to attain sufficient signal-to-noise ratio. The induced FCA transient at different depths was measured at the injection level varied from 10^{17} cm^{-3} to $8{\cdot}10^{18}$ cm^{-3}. Due to dominating absorption cross-section $\Delta\alpha(t)$ and a fast capture of minority hole to the deep traps, the decay mainly reflects the free excess electron absorption in the conduction band.

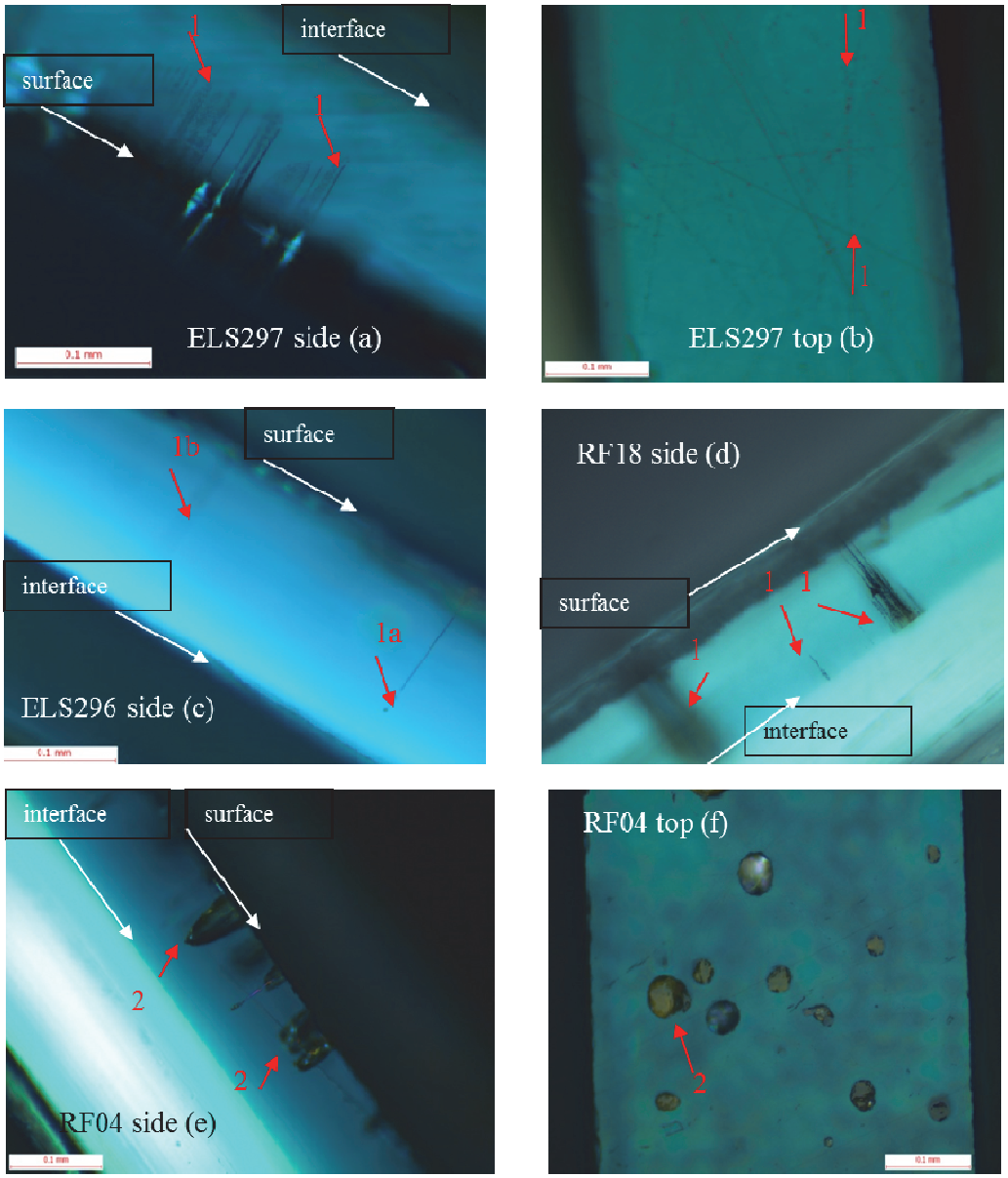

Figure 1. Nomarsky optical images of co-doped 6H-SiC in crossed polarized field (a, c, d, e – side view and b, f – top view); a bar for all pictures is equal to 100 μm. White arrows mark the "interface" between epilayer/substrate and the outer "surface". Red arrows indicate (1) - thin carbon filamentary inclusion, and (2) - polycrystalline cone inclusion. In (a) the colonies of filamentary inclusions are originating from the mid of epilayer thickness. In (c) one filamentary carbon inclusion (1a) is well focused while the other (1b) is out of a focal plane. In (d) the cone shape defects are starting at the interface (the near surface range is unrevealed due to unfinished polishing) and in (e) they appear further within the epilayer. In (f) the polycrystalline inclusions are visible on a top-epi view.

3. Main Results and Discussion

Figures 2a, 2b show the extracted $\Delta\alpha(t)$ depth-distributions in two samples at different time, *t,* after the laser pulse. At t = 10 ns, an exponential slope from the excited surface originates which can be explained by the absorption generated electron-hole pairs. Band-to-band absorption coefficient value is obtained from the slope (dashed line) is α_{bb} = 900 cm^{-1} which is very close to value of 1000 cm^{-1} reported for undoped 6H-SiC at the same 355 nm excitation wavelength [7]. This shows that band gap absorption is little affected by high co-doping. At the later μs-long time-span, substantial smoothening in the FCA carrier profiles is observed. From the results in figure 1a, b we may conclude that the diffusion driven surface recombination on the excited surface remains small or almost insignificant. This is based on the observation that, at further elapsed times, no carrier gradient arises towards the surface. Low diffusivity is also confirmed by the fact that FCA did not exceed the generation slope on a straight dashed line. These findings are in contrast to substantial ambipolar carrier diffusion phenomenon observed in undoped 6H-SiC [7]. Therefore, the low values of ambipolar diffusion coefficient D = 0-0.1 cm^2/s have been extracted in heavily co-doped SiC by transient grating measurements reported in this issue [see Gulbinas K et al. this issue]. It was shown that, at injection level approaching the concentration of boron, D value start to increase. This most probably promotes easy access for carriers to the recombination centers therefore lifetime decreases.

The injection dependence of the carrier lifetimes in RF18 sample is shown in figure 2c. The FCA amplitude saturation is observed at the 10 μm probe depth at 1 mJ/cm^2 excitation fluence (see inset) which correspond to injected carrier density of about 5·10^{18} cm^{-3}. The saturation can be attributed to the fact that carrier lifetime becomes shorter than the excitation pulse (τ_R < 2 ns). The FCA smoothing in figure 2a, b is resulting from pronounced injection dependence of the electron lifetime between 2 ns and 1-3 μs.

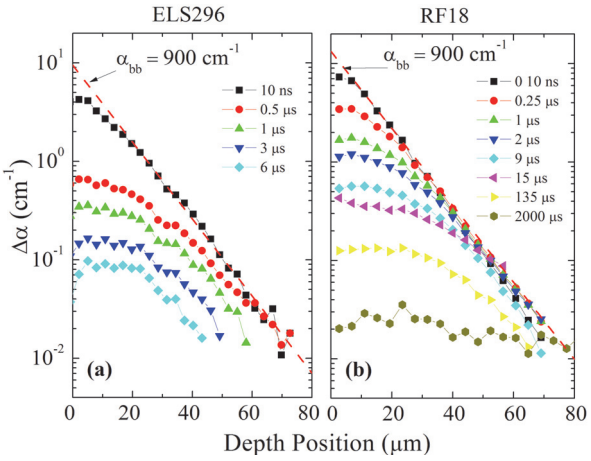

Figure 2a, b Depth-distributions of FCA in two samples at different time after exciting laser pulse.

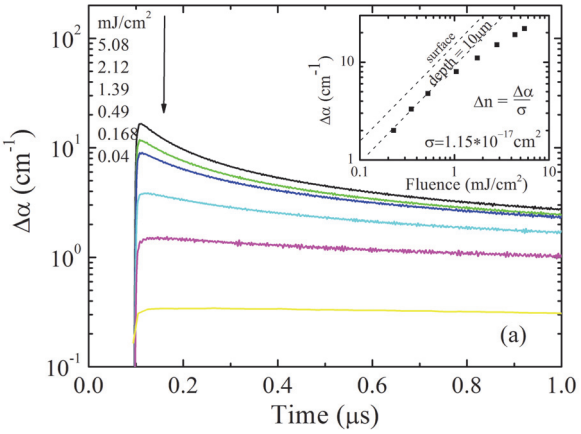

Figure 2c. Induced FCA transients and amplitude (inset) at different excitation fluence in the depth position of 10 μm from the excited surface in RF18 sample. Note that carrier lifetimes are injection dependent.

Figure 3a shows the comparison of $\Delta\alpha(t)$ transients in different samples on a double-log plot at the medium carrier injection of about >10^{17} cm^{-3}. Quite short almost exponential carrier lifetime 0.1-0.18 μs is detected in the high defected samples ELS297 and RF04. While, in two low defective samples (ELS296 and RF18), the carrier lifetime is substantially longer and exhibits components including two extending ones from 50 μs to 1.2 ms. These components are marked by fitted dashed lines in figure 2c. In RF-batch samples the short sub-μs lifetime 0.22 and 1.5 of about same value has been detected by microwave photoconductivity decay at lower injection level of about 10^{16} cm^{-3} (see table 1). This confirms that influence of in-grown defects is related to short carrier lifetime at any external injection provided.

We have performed time-integrated DAP photoluminescence study by excitation with 355 nm 25 ps pulses. At room temperature, PL DAP emission was observed in two samples RF18 and ELS296 containing long carrier lifetimes. However, no PL emission was detected in two samples RF04 and ELS297 with a short lifetime. Since it is known that DAP radiative recombination times are fairly long, appearing on a ms-scale [1], it can be concluded that a short nonradiative carrier lifetime which is related to the grown-in defects prevents DAP emission probability. The investigation of carrier lifetime temperature dependences in a similarly co-doped sample (ELS118: $d_{epi} \approx 45$ μm, N = $9.2 \cdot 10^{18}$ cm^{-3}, B = $5.2 \cdot 10^{18}$ cm^{-3}) has been performed in the orthogonal FCA measurement geometry [Manolis et al. this issue]. It allowed distinction of three recombination paths for free electrons. In figure 3b these relaxation processes are presented schematically. The main non-radiative path is through the $Z_{1/2}$ (carbon vacancy) with microsecond lifetime (figure 3b), thus, it is suppressed due to strongly restricted diffusivity of the free carriers in a heavily co-doped 6H-SiC.

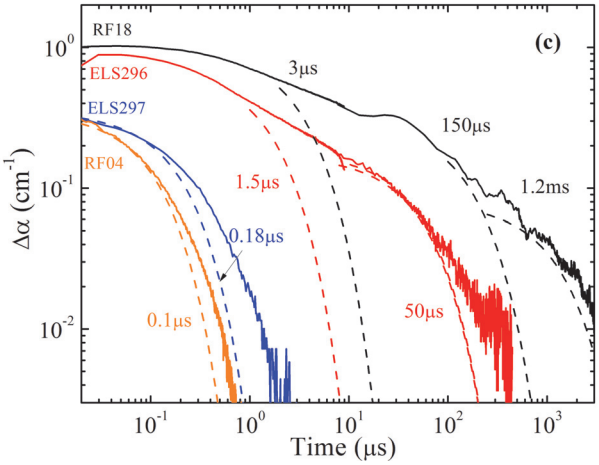

Figure 3a. FCA transients on a double-log scale in four samples at 300 K. Exponential fits are provided by dashed curve with a value of the carrier lifetime.

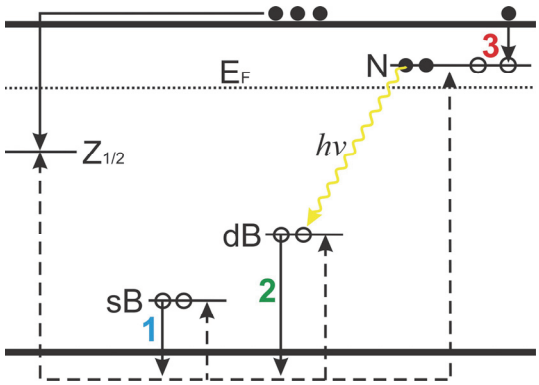

Figure 3b. Schematic of DAP radiation with carrier's release of holes from shallow and deep Boron and to recombination through N sites. Competing recombination channel through $Z_{1/2}$ center is also indicated.

4. Conclusion

The carrier lifetime depth distribution in co-doped B-N 6H-SiC shows that, even at high injection level, the surface recombination driven by carrier diffusion is small and negligible. However due to diffusion increase with injection density the carrier access to the non-radiative centers increases and carrier lifetime obey a drop. This occurs for injection of minority hole density exceeding density of acceptor levels. To achieve efficient DAP luminescence in co-doped samples the ms-long carrier lifetimes are needed. This can be optimized by balancing the doping and improving the crystal quality of the material.

Acknowledgement. This research was supported by Swedish Visby program grant No 00729/2010.

References

[1] Sun J W, Kamiyama S, Jokubavicius V, Peyre H, Yakimova R, Juillaguest S, and Syväjärvi M 2012 *J. Phys. D: Appl. Phys.* **45** 235107
[2] Kamiyama S, Iwaya M, Takeuchi T, Akasaki I, Syväjärvi M, and Yakimova R, 2011 *J. Semicond*. **32** 013004
[3] Kamiyama S, Maeda T, Nakamura Y, Iwada M, Amano H, Akasaki I, Kinoshita H, Furusho T, Yoshimoto M, Kmoto T, Suda J, Henry A, Ivanov I G, Bergman J P, Monemar B, Onuma T, and Chichibu S F 2006 *J. Appl. Phys*. **99** 093108

[4] Syväjärvi M, Müller J, Sun J W, Grivickas V, Ou Y, Jokubavicius V, Hens P, Kaisr M, Ariyawong K, Gulbinas K, Liljedahl R, Linnarsson M K, Kamiyama S, Wellmann P, Spiecker E and Ou H 2012 *Physica Scripta* **T148** 014002
[5] Duijn-Arnold A V, Icoma T, Poluektov O G, Baranov P G, Mokhov E N and Schmidt J 1998, *Phys. Rev.* B **57** 1607-19
[6] Grivickas V and Linnros J 2012 "Carrier lifetime: Free carrier absorption, photoconductivity and photoluminescence" Chapter in the book „*Characterization of Materials*" Second Ed. 3 volums (John Viley & Sons, Inc. US) Ed. Kaufmann E N Vol. 1 pp. 658-692
[7] Galeckas A, Linnros J, Frischholz M, and Grivickas V 2001 *Appl. Phys. Lett.* **79** 365-367